ISSN 2321-807X
Volume 12 Number12
Journal of Advances in chemistry

Effect of N-(6-aminobenzo[d]thiazol-2-yl)benzamide and 2,6-diamino-benzothiazole as Corrosion Inhibitor in acid medium

Rekha.S*, Kannan.K, Gnanavel.S
Department of chemistry,Knowledge Institute of Technology, Salem, Tamilnadu, India.
E-mail- chemist.rekha@gmail.com
Department of Chemistry, Government College of Engineering, Salem, Tamilnadu, India
E-mail-kannan_k2002@yahoo.co.in

ABSTRACT

2-amino-6-nitrobenzothiazole(ANBT) was used as an inhibitor for the corrosion of mild steel in acid medium since the inhibition efficiency was low for that compound, 2,6-diaminobenzothiazole (DABT) and N-(6-aminobenzo [d] thiazol-2-y1) benzamide(ABTB) was synthesized, and characterized by FT-IR, H^1NMR, and C^{13}NMR.The synthesized compound was tested as a corrosion inhibitor for mild steel in 1N HCl solution using weight loss, Potentiodynamic polarization, and AC impedance techniques. The inhibition efficiency was studied at the different time, temperature and acid concentration by weight loss method. The values of activation energy and free energy of adsorption of these compounds were also calculated, which reveals that the inhibitor was adsorbed on the mild steel by physisorption mechanism. Adsorption obeys Langmuir and Temkin adsorption isotherms. The results obtained by weight loss method revealed that the compound performed as a better inhibitor for mild steel in 1N HCl. Potentiodynamic polarization studies showed that the inhibitor acts as a mixed type inhibitor.AC impedance studies revealed that the corrosion process was controlled by charge transfer process. Surface analysis was studied using SEM and FT-IR.

Keywords: Mild steel, weight loss, Potentiodynamic polarization, AC impedance, SEM

Academic Discipline And Sub-Disciplines

Chemistry/Electrochemistry

SUBJECT CLASSIFICATION

Corrosion

TYPE (METHOD/APPROACH)

Experimental study

1. INTRODUCTION

Corrosion of mild steel in acid medium is one of the major problems in most of the industries especially in the case of petroleum industries, pharmaceutical companies, oil refineries and food industries[1].There are many methods available to prevent and control the corrosion of the metal in acid medium, but the most promising technology is the use of inhibitors[2,3]. Many authors proved that the heterocyclic compounds containing N, S, O, and P has excellent inhibition property in addition to double bonds due to the adsorption process which acts as a physical barrier between the metal and the acid medium[4]. Even though many heterocyclic compounds have been reported as an efficient inhibitor in acid medium, the heterocyclic compound having sulphur and nitrogen has received only minor attention. Finally, literature survey revealed the better corrosion inhibition effect of benzothiazole derivatives for mild steel, copper and zinc corrosion in acidic medium[5-9]. Recently many benzothiazole derivatives have been studied as corrosion inhibitors for mild steel, and they have shown excellent results[10-12]. But, even now nobody has studied the effect of 2-amino-6-nitrobenzothiazole has not yet been investigated as inhibitors for the corrosion of mild steel in acidic solutions. In continuation of the present work, we have studied the inhibition efficiency of 2-amino-6-nitrobenzothiazole and synthesized 2,6-diamino-benzothiazole, N-(6-aminobenzo [d] thiazol-2-y1) benzamide for the corrosion of mild steel in 1N HC1 solution by using techniques such as weight loss. Then efficiency of the better inhibition inhibitors was studied by weight loss method with various parameters, Potentiodynamic polarization and AC impedance.

2.EXPERIMENTAL

2.1 Materials and Characterisation:

For the synthesis of 2,6-diamino-benzothiazole, N-(6-aminobenzo [d] thiazol-2-y1) benzamide, 2-amino-6-nitrobenzothiazole, THF, Triethyl amine, benzoyl chloride, HCl, $SnCl_2$, Methanol, Zn dust and Ammonium formate were used.(Sigma and Aldrich products).The chemical structure of 2,6-diamino benzothiazole and N-(6-aminobenzo [d] thiazol-2-y1) benzamide were characterized using FT-IR(JASCO FT-IR 430 spectrophotometer in KBr pellet), H^1NMR and C^{13}NMR(Bruker AC 300F (300MHz)). For these studies, we used DMSO as an solvent , and TMS as an internal standard.

2.1.1 Synthesis

(i) Synthesis of 2,6diaminobenzothiazole:

1g of **2-amino-6-nitrobenzothiazole** dissolved in 12 N HCl (12ml) was taken in a round bottom flask fitted with the magnetic stirrer. To the resulting suspension **$SnCl_2$** (9g) was added in portion wise at room temperature for every half an hour and the reaction mass was stirred at room temperature for 1.5 hr. The reaction mass was slowly poured onto crushed ice mixed with water and neutralized by adding 40% NaOH (pH = 7 to 8). The off-white solid formed was extracted with ethyl acetate. The organic layer was separated, and the aqueous layer was extracted with ethyl acetate. Then it was washed with brine solution and dried over anhydrous sodium sulfate, and concentrated under reduced pressure using rotary evaporator. The crude residue was recrystallized with diethyl ether to afford purified **2,6-diaminobenzothiazole.** Melting point -205°C. The purity was checked using Thin Layer Chromatography. The compound was confirmed through FT-IR, H^1NMR, and C^{13}NMR spectrum.

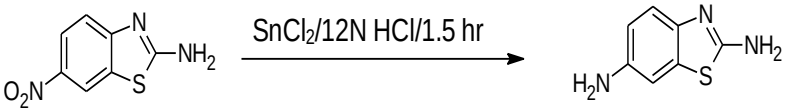

(ii)Synthesis of N-(6-aminobenzo[d]thiazol-2-yl)benzamide:

Step-I: Synthesis and characreistion of N-(6-nitrobenzo[d]thiazol-2-yl)benzamide.

A 250 ml round bottom flask fitted with magnetic stirrer was charged with 2-amino-6-nitrobenzothizole (10g, 0.050mol) in THF (100 ml).To the above said reaction mass Triethyl amine (21 ml, 0.153mol) followed by Benzoyl Chloride (9.13ml,0.128mol) was added at 0°C, and the resulting suspension was stirred at RT for 12 hours. The reaction mass was poured into water, the pale yellow solid formed was extracted with ethyl acetate. The organic layer was separated, and the aqueous layer was extracted with ethyl acetate (2x150ml). The combined organic layers were washed with 2N HCl (2x200ml), brine solution (1x300ml) and dried over anhydrous sodium sulfate. Then the organic layer obtainedwas concentrated under reduced pressure. The crude residue recrystallized with Diethyl ether to afford 7g (56%) of the product. The purity was checked by thin layer chromatography. The compounds were confirmed by FT-IR, H^1NMR and C^{13}NMR.

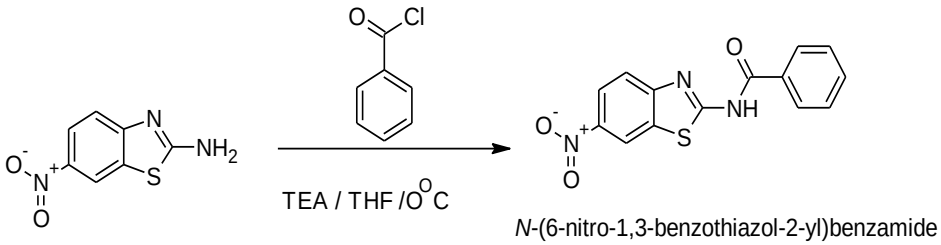

N-(6-nitro-1,3-benzothiazol-2-yl)benzamide

Step-II :Synthesis and characreistion of N-(6-aminobenzo[d]thiazol-2-yl)acetamide.

N-(6-nitrobenzo[d]thiazol-2-yl)benzamide(5g,0.012mol) was taken in 100ml of Methanol solution in a 100 ml round bottom flask fitted with the magnetic stirrer. To the reaction mass Zn dust (6.8g,0.105mol) was added at 0°C. Then to the resulting suspension Ammonium Formate (6.9g,0.105mol) was added in portion wise, and the reaction mass was stirred at RT for 2 hr. The reaction mass was slowly poured onto crushed ice mixed with water. The off- white solid formed was extracted with ethyl acetate. The organic layer was separated, and the aqueous layer was extracted with ethyl acetate (2x125ml). The combined organic layers were washed with brine solution (1x250ml), dried over anhydrous sodium sulfate, and concentrated under reduced pressure. The crude residue was recrystallized with Diethyl ether to afforded 1.43g (54%) of product. The purity was checked by thin layer chromatography. The compounds were confirmed by FT-IR, H^1NMR, and C^{13}NMR.

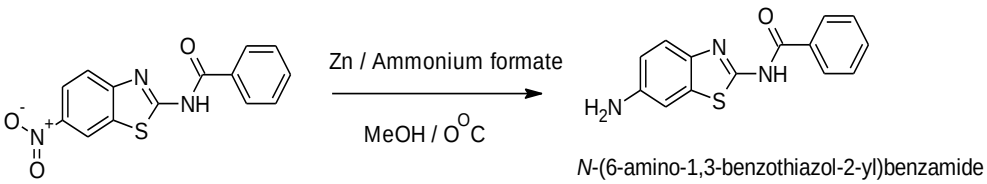

N-(6-amino-1,3-benzothiazol-2-yl)benzamide

2.1.2 TLC Analysis:

The crude sample and the purified sample were dissolved in ethyl acetate, and it was spotted on the TLC plate. The spotted TLC plate was developed in the chloroform: methanol(9:1) solvent mixture system and then it was dried. The dried TLC plate was immersed in the iodine vapour tank for about 5 min to visualize the various spots developed.

2.1.3 Structural Elucidation:(FT-IR,H^1NMR, and C^{13} NMR)

The FT-IR spectra were recorded on a JASCO FT-IR 430 spectrophotometer in KBr pellet. H^1NMR and C^{13}NMR spectra were recorded using Bruker AC 300F (300MHz) NMR spectrophotometer. For these studies, DMSO was used as the solvent, and TMS was used as an internal standard.

2.2 Corrosion Inhibition Measurements.

2.2.1.Weight loss studies:

The weight loss studies have been carried out using a glass beaker containing 100ml test solution of 1N HCl. The mild steel specimen was cleaned, weighed, and it was immersed in the test solution by hanging from the glass rod using Teflon thread. After one hour of immersion, the electrode was withdrawn, rinsed with double distilled water, washed with acetone, dried and weighed. The same procedure was followed for the experiments in 1N HCl solution for different concentration of the inhibitor (100-1100ppm), acid concentration (1, 3, 5 N), time intervals (1-7hours), and temperature (303, 313, 323, 333 K). From the weight loss of the mild steel specimen, the corrosion rate, the inhibition efficiency and the surface coverage of the metal surface was calculated using the following formulas

$$\text{Corrosion rate} = \frac{87.5 \times \text{loss of weight}}{\text{Density} \times \text{Area (cm}^2\text{)} \times \text{time of exposure}} \text{ mmpy} \quad \text{----------} \rightarrow (1)$$

$$\text{Surface Coverage } (\Theta) = \frac{W_U - W_I}{W_U} \quad \text{----------} \rightarrow (2)$$

Here Wu and Wi are the change in weight of the mild steel specimen in the absence and presence of inhibitor(same temperature)

$$\text{Inhibition efficiency} = \frac{Wu - Wi}{Wu} \times 100 \quad \text{----------} \rightarrow (3)$$

2.2.2 Potentiodynamic Polarisation and AC Impedance Studies:

Electrode surface preparation: A rod made up of mild steel of the same composition embedded with Teflon with an exposed area of 0.8113inch2 was polished using emery papers of grade1/0,2/0,3/0 and 4/0 and finally cleaned with trichloroethylene and then used for the experiments used for carrying out the electrochemical measurements.In this studies, a rod made up of mild steel was used as the working electrode; the saturated calomel electrode, was used as a reference electrode and a rectangular platinum foil was used as a counter electrode. The solution capacity is 100ml.

Electrochemical study: Electrochemical instrument unit (CHI608E) was used for conducting Electrochemical Impedance Spectroscopy (EIS) and Tafel polarization studies. The EIS measurements were carried out at corrosion potential range of frequency 10 kHz to 0.01 kHz with signal amplitude of 10 m V. The Tafel polarization measurements were made for a potential range of -200 m V to +200 m V with respect to open circuit potential, at a scan rate of 1 m V/sec. The I_{corr}, E_{corr}, R_{ct} and C_{dl} values were obtained from the data of the corresponding “Corr view” and “Z View” software. The inhibition efficiency for potentiodynamic polarization studies was calculated from the value of I_{corr} using the formula.

$$\text{I.E (\%)} = \frac{I_{corr\,(blank)} - I_{corr(inh)}}{I_{corr(bank)}} \times 100 \quad \text{----------} \rightarrow (4)$$

The inhibition efficiency of the impedance measurements was calculated using the formula

$$\text{I.E (\%)} = \frac{R_{ct(inh)} - R_{ct(blank)}}{R_{ct\,(inh)}} \times 100 \quad \text{----------} \rightarrow (5)$$

$R_{ct\,(inh)}$ is the charge transfer resistance with inhibitor.

$R_{ct\,(blank)}$ is the charge transfer resistance without inhibitor.

2.2.3 Surface Morphology

Surface morphology was examined using SEM and IR in the presence and absence of inhibitor

ISSN 2321-807X
Volume 12 Number12
Journal of Advances in chemistry

3. RESULTS AND DISCUSSION

3.1. Characterisation of DABT and ABTB

3.1.1 Characterisation of 2,6-diamino-benzothiazole (DABT)

The proposed structure of 2,6-diamino-benzothiazole (DABT) given in Figure 1 was confirmed from the FT-IR and NMR spectral data which are given below. The data obtained from these spectra were discussed in a detailed manner.

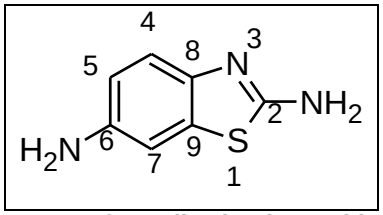

Figure 1. Structure of 2,6-diamino-benzothiazole (DABT)

FT-IR spectrum of DABT is shown in Figure 2. The peak values of the IR spectra and their assignments are shown in Table 1. The assignment of peaks appeared in various region of FT-IR spectrum to the functional groups present in the inhibitor DABT are represented as follows: a sharp peak at 1613.37cm^{-1} is due to1° amine, a peak at 3098 cm^{-1} is assigned to Aromatic=CH (stretching), peak at 1547.58 cm^{-1} is attributed to C=C group in the aromatic ring, peak at

3.1.1.1 FT-IR spectral analysis

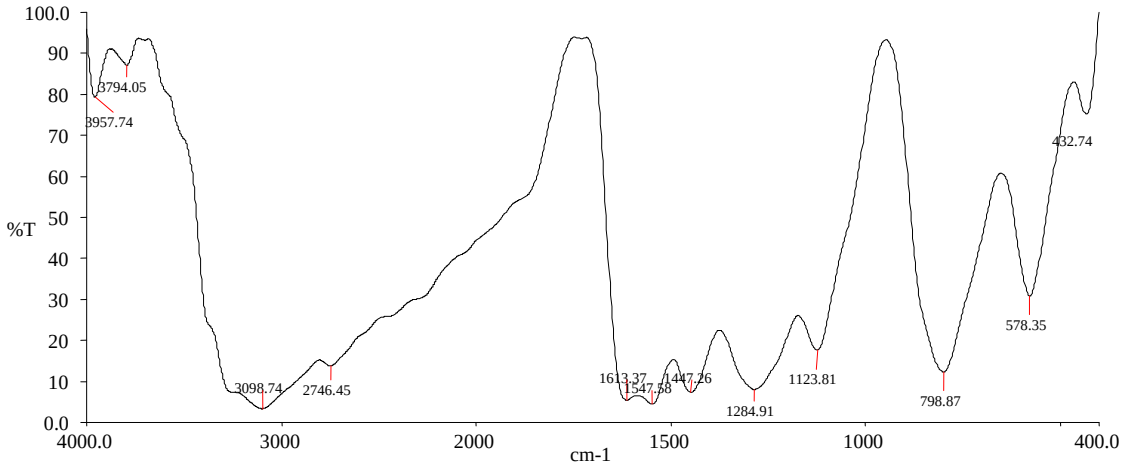

Figure 2. FT-IR spectrum of 2,6-diamino-benzothiazole (DABT)

798.87 cm^{-1} is due =CH (bending) group in the inhibitor. It could be confirmed from the result that the inhibitor contains primary amine and an aromatic ring.

Table.1 FT-IR spectral data of 2,6-diamino-benzothiazole (DABT)

Peak Value(cm^{-1})	Possible groups
1613.37	1° amine
3098	Aromatic=CH (stretching)
1547.58	Aromatic C=C (stretching),
798.87	=CH (bending)

3.1.1.2 NMR spectral analysis

3.1.1.2.1 ^{1}H NMR spectral analysis

^{1}H NMR spectrum of DABT is shown in Figure 3. The peak values of the spectra and their assignments to various proton environments in the inhibitor molecule are shown in Table 2. The singlet at 4.79 ppm to two hydrogen atoms in the amine group attached to carbon labeled as 2, doublet at 6.47-6.51 ppm is assigned to one hydrogen labeled as 4, doublet at 6.80-6.81 ppm is assigned to one hydrogen labeled as 5.The singlet at 6.94 ppm is assigned to two hydrogen atoms labeled as 6, singlet at 7.05 ppm is assigned to one hydrogen labeled as 7. The structure of the inhibitor was clearly confirmed by resulting above data. The chemical shift for Proton 6 with broad splitting clearly indicates that there is formation of amine product.

Table 2 ^{1}H NMR-analysis of 2,6-diamino-benzothiazole (DABT)

Peak value (δ) ppm	Peak type	No.of Hydrogen atoms assigned	Position in the structure
4.79	Singlet	2	2
6.47-6.51	Doublet	1	4
6.80-6.81	Doublet	1	5
6.94	Singlet	2	6
7.05	Singlet	1	7

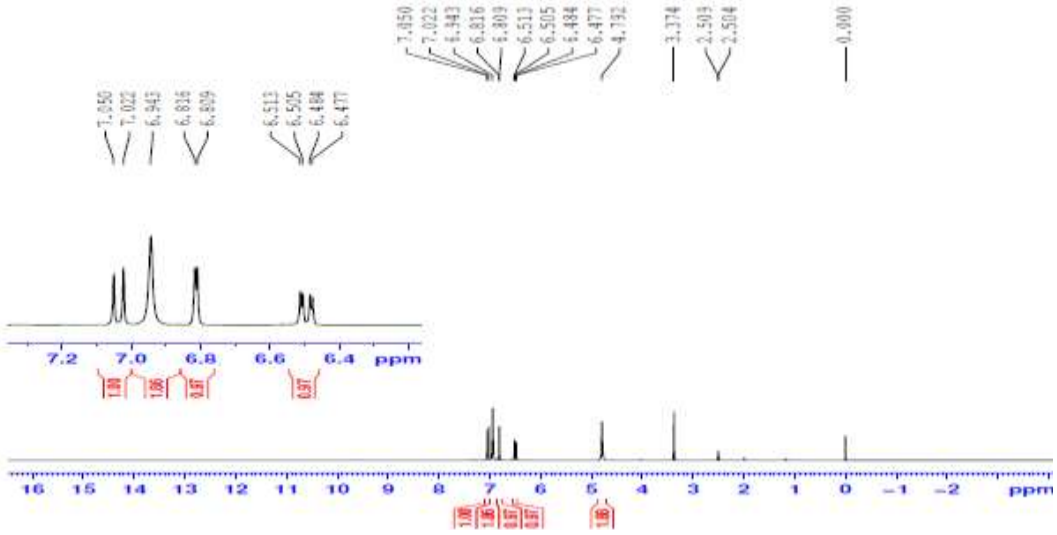

Figure 3 H^{1}- NMR spectrum of 2,6-diamino-benzothiazole (DABT)

3.1.1.2.2 ^{13}C NMR spectral analysis

^{13}C NMR spectrum of DABT is shown in Figure 4. The peak values of the spectra and their assignments to various carbon environments in the inhibitor molecule are shown in Table 3. The singlet at 105.27 ppm is assigned to carbon atom labeled as 7, singlet at 112.8 ppm is attributed to carbon atom labeled as 5, singlet at 117.9 ppm is referred to carbon atom labeled as 4, singlet at 131.8 ppm is assigned to carbon atom labeled as 9, singlet at 143.3 ppm is attributed to carbon atom labeled as 8, singlet at 143.7 ppm is assigned to carbon atom labeled as 6, singlet at 162.2 ppm is referred to carbon atom labeled as 2. The structure of the inhibitor was clearly confirmed by resulting data of the FT-IR and NMR spectrum.

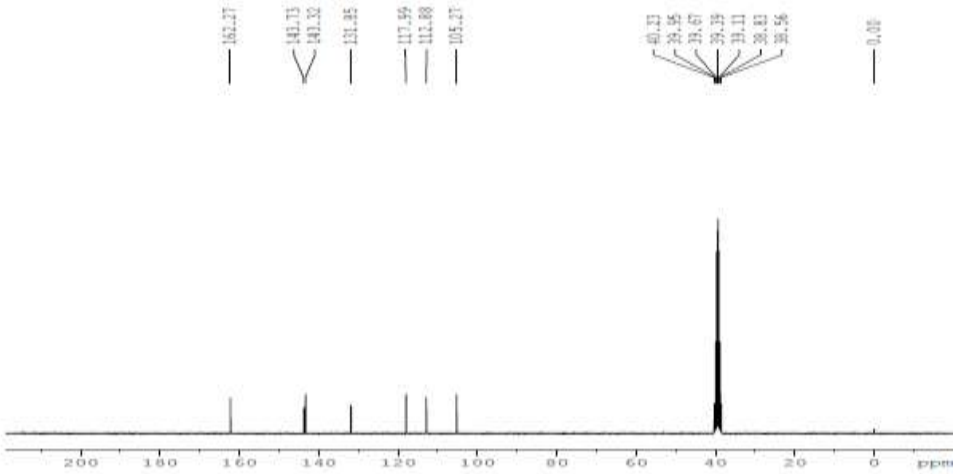

Figure 4. ^{13}C- NMR spectrum of 2,6-diamino-benzothiazole (DABT)

Table 3 ^{13}C-NMR spectral data of 2,6-diamino-benzothiazole (DABT).

Peak value(δ) ppm	Peak type	No:of carbon assigned	Position in the structure
105.27	Singlet	1	7
112.8	Singlet	1	5
117.9	Singlet	1	4
131.8	Singlet	1	9
143.3	Singlet	1	8
143.7	Singlet	1	6
162.2	Singlet	1	2
163.37	Singlet	1	2
70.11	Singlet	1	9

3.1.2 Characterisation of 6-aminobenzo[d]thiazol-2-yl)benzamide (ABTB)

The inhibitor molecule was synthesized in two steps.So the characterization of N-(6-aminobenzo[d]thiazol-2-yl) benzamide includes the characterization of the intermediate product. Newly synthesized N-(6-nitrobenzo[d]thiazol-2-yl)benzamide obtained in step-I and N-(6-aminobenzo[d]thiazol-2-yl)benzamide**(ABTA)** inhibitor molecule were characterized using the following data obtained from FT-IR and NMR spectrum.

3.1.2.1 FT-IR Spectral Analysis

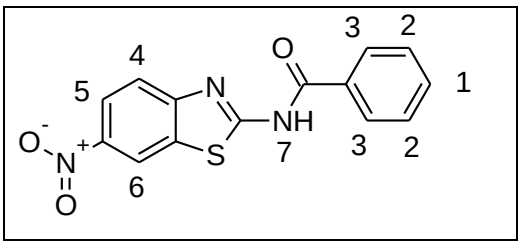

Figure 5 Structure of N-(6-nitrobenzo[d]thiazol-2-yl) benzamide for FT-IR analysis

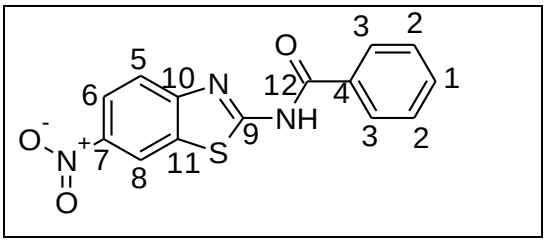

Figure 6 Structure of N-(6-aminobenzo[d]thiazol-2-yl) benzamide for FT-IR analysis

3.1.2.1.1 FT-IR analysis of N-(6-nitrobenzo[d]thiazol-2-yl) benzamide

The FT-IR spectral data of N-(6-nitrobenzo[d]thiazol-2-yl) benzamide are shown in Table 4. The recorded spectrum was shown in Figure 7. The assignment of peaks appeared in various regions of FT-IR spectrum of the functional groups present in the inhibitor are represented as follows: a sharp peak appeared in the area 3434.25cm^{-1} is attributed to amide group, the peak at 2827.62cm^{-1} is due to the –C-H- group in the aromatic ring and the sharp peak appeared in the region of 1595.81cm^{-1}is attributed to the C=O attached to amide group. The peaks at 1447.48cm^{-} is due to the –C=C- in the aromatic ring. The peak appeared in the region of 1353.14cm^{-1}is due to the Nitro group in the structure.The peak in the region 683.63 is due to the Aromatic monosubstitution (C-H deforming). It could be confirmed from the table that the compound contains nitro, amide, methyl and aromatic ring as shown in Figure 7.

Table 4 FT-IR spectral data of 6-nitrobenzo[d]thiazol-2-yl)benzamide

Peak Value(cm^{-1})	**Possible groups**		**Peak Value(cm^{-1})**	**Possible groups**
3434.25	Amide		1447.48	–C=C- group in the aromatic ring
2827.62	–C-H- group in the aromatic ring		1353.14	Nitro
1595.81	C=O attached to amide group		683.63	Aromatic monosubstitution (C-H deforming)

3.1.2.1.2 FT-IR analysis of N-(6-aminobenzo[d]thiazol-2-yl) benzamide

The FT-IR spectral data of N-(6-aminobenzo[d]thiazol-2-yl) benzamide are shown in Table 5. The recorded spectrum was shown in Figure 8. The assignment of peaks appeared in various regions of FT-IR spectrum for the functional groups present in the inhibitor are represented as follows: a sharp peak appeared in the region 3399.60cm^{-1} are attributed to amine group., the peak at 3298 cm^{-1} is assigned to the amide group, and the sharp peak appeared in the area of 3321.33cm^{-1}is attributed to the methyl group. The peak appeared in the region of 3063.47cm^{-1}is due to –C-H- groups in the aromatic ring and the peak at 1659.05 cm^{-1} is due to C=O attached to amide group, and the peaks at 1464.72cm^{-1} is attributed to the –C=C- groups in the aromatic ring and the peaks at 698.03 cm^{-1}is due to the aromatic monosubstitution (C-H deforming) . It could be confirmed from the table that the compound contains amine, amide, methyl and aromatic ring as shown in Figure 6.

Table 5. FT-IR spectral data of N-(6-aminobenzo[d]thiazol-2-yl) benzamide

Peak Value(cm^{-1})	Possible groups		Peak Value(cm^{-1})	Possible groups
3399.60	Amine		1659.05	C=O attached to amidegroup
3321.33	Amide		1464.72	–C=C- group in the aromatic ring
3063.47	–C-H- group in the aromatic ring		698.03	Aromatic monosubstitution (C-H deforming)

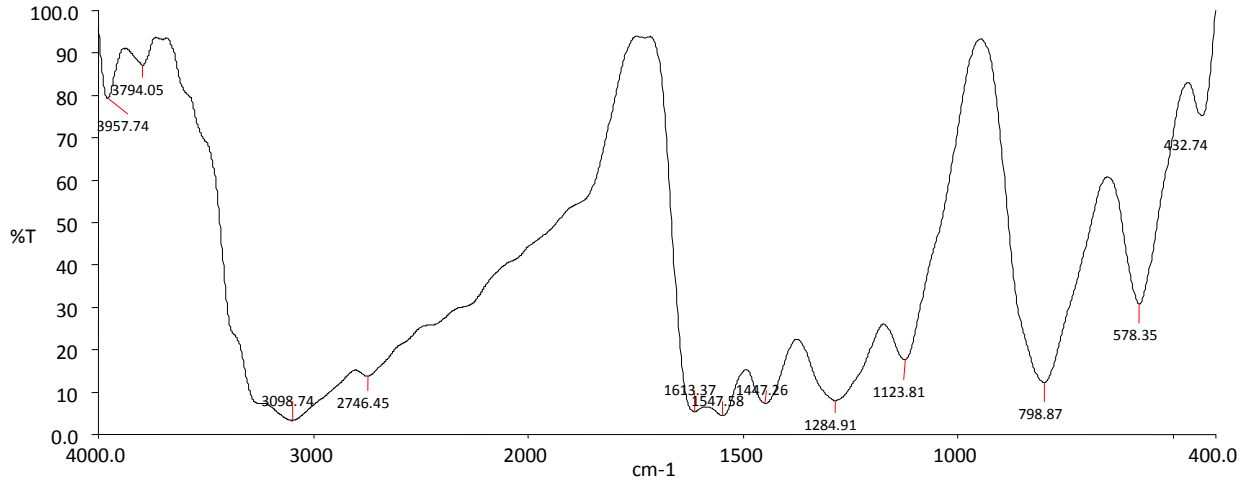

Figure 7 FT-IR spectrum of N-(6-nitrobenzo[d]thiazol-2-yl) benzamide.

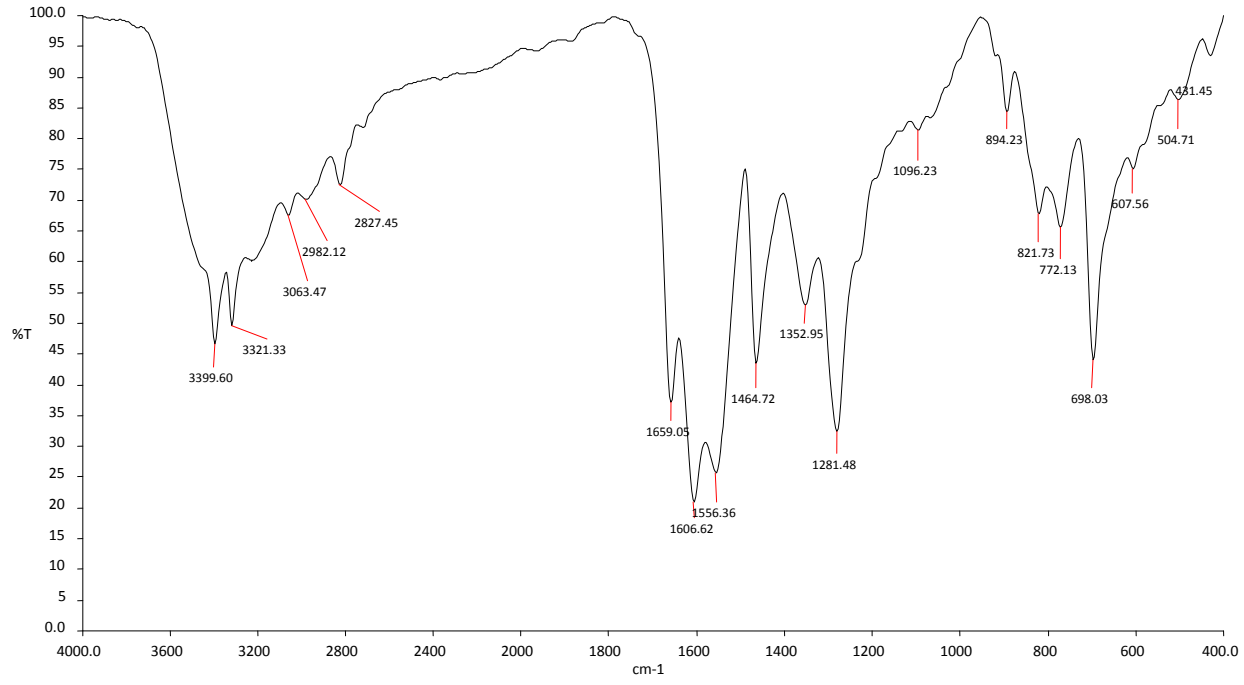

Figure 8. FT-IR spectrum of N-(6-aminobenzo[d]thiazol-2-yl) benzamide

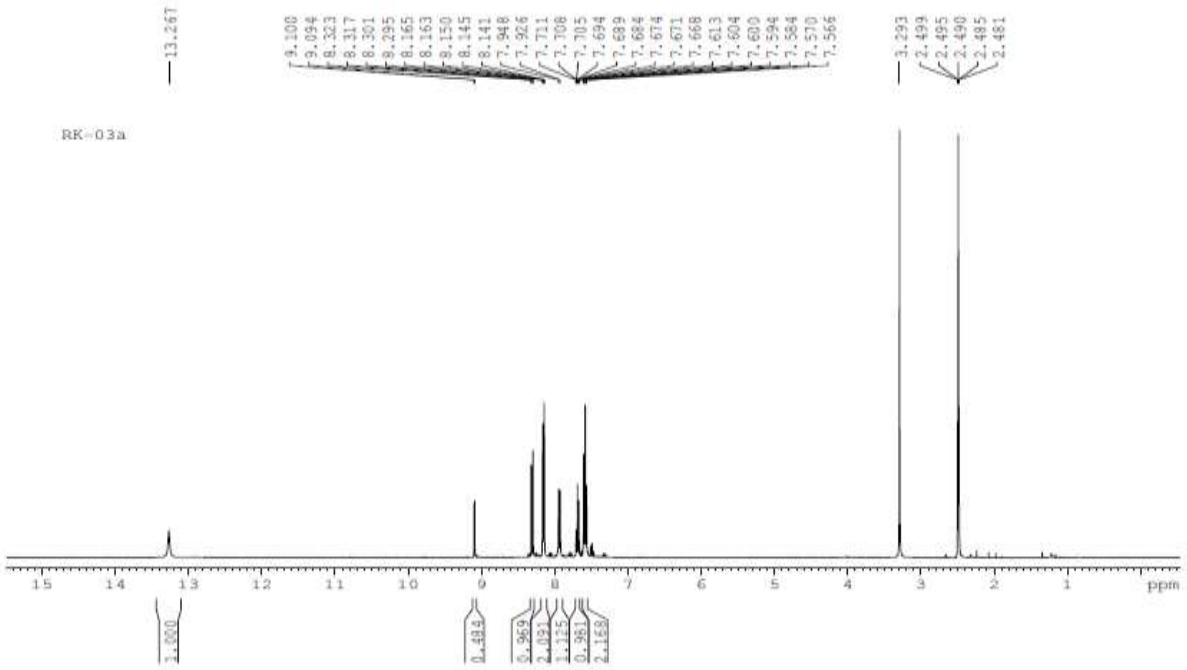

Figure 9. H[1]- NMR spectrum of N-(6-nitrobenzo[d]thiazol-2-yl) benzamide

3.1.2.2 NMR Spectral Analysis

3.1.2.2.1 [1]H NMR-Analysis of N-(6-nitrobenzo[d]thiazol-2-yl) benzamide

The structure was confirmed by [1]H NMR [200 MHz, DMSO-d6].The [1]H NMR spectral data of N-(6-nitrobenzo[d]thiazol-2-yl)benzamide are given in Table 6. The recorded spectrum was shown in Figure 9. Triplet at 7.66-7.71 is assigned to one hydrogen atoms labeled as 1, Multiplet at 7.56-7.61 is attributed to two hydrogen atoms labeled as 2, doublet at 8.14-8.16 is assigned to 2 hydrogen atom labelled as 3, doublet at 8.29-8.32 is attributed to one hydrogen atom labeled as 4, doublet at 7.93 is assigned to one hydrogen atom labeled as 6, doublet at 9.10 is assigned to one hydrogen atom labeled as 6, singlet at 13.26 is attributed to one hydrogen atom labeled as 7.

Table 6. [1]H NMR-analysis of N-(6-nitrobenzo[d]thiazol-2-yl) benzamide

Peak value (δ) ppm	Peak type	No.of Hydrogen atoms assigned	Position in the structure
7.66-7.71	Triplet	1	1
7.56-7.61	Multiplet	2	2
8.14-8.165	Doublet	2	3
8.29-8.32	Doublet	1	4
7.93	Doublet	1	5
9.10	Doublet	1	6
13.26	Singlet	1	7

3.1.2.2.2 [1]H NMR-Analysis of N-(6-aminobenzo[d]thiazol-2-yl) benzamide

The structure of ABTB was confirmed by[1]H NMR [200 MHz, DMSO-d6]. The [1]H NMR spectral data are presented in Table 7. The recorded spectrum was shown in Figure 10. The doublet at 7.44 ppm is assigned to one hydrogen atoms labeled as 1, triplet at 7.51-7.55 ppm is assigned to two hydrogens numbered as 2, doublet at 8.10 ppm is attributed to two hydrogens marked as 3, triplet at 7.6-7.65 ppm is assigned to one hydrogen atoms labeled as 4, doublet at 6.71-6.74 ppm is assigned to one hydrogen atoms labeled as 5, doublet at 7.03 ppm is attributed to one hydrogen atoms labeled as 6. The singlet at 5.18 is attributed to two carbon atom labled as 7, singlet at 12.51 is assigned to one hydrogen atom labeled as 8. The structure of the N-(6-aminobenzo[d]thiazol-2-yl)acetamide was evidently confirmed by the resulting data that is given above.

ISSN 2321-807X
Volume 12 Number12
Journal of Advances in chemistry

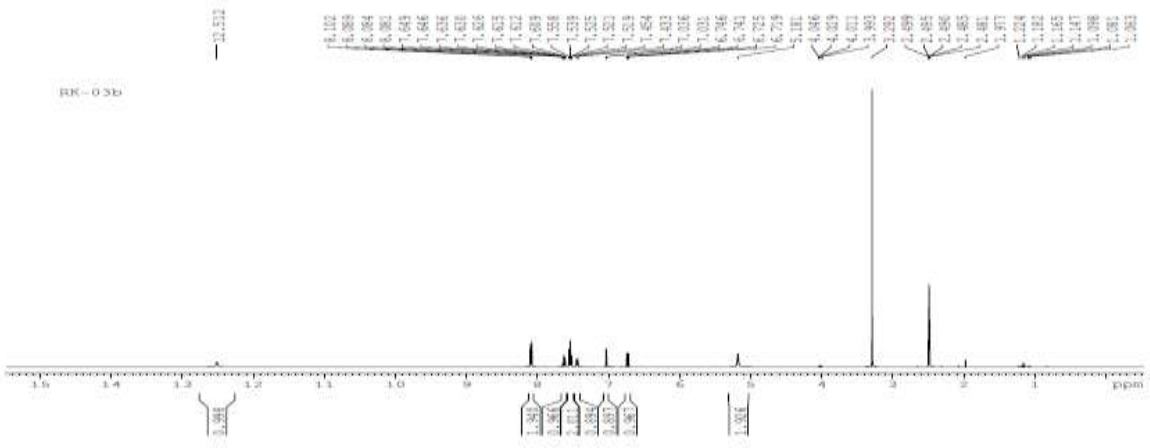

Figure 10. H^1- NMR spectrum of N-(6-aminobenzo[d]thiazol-2-yl) benzamide

Table 7. ^{1}H NMR spectral data of N-(6-aminobenzo[d]thiazol-2-yl)benzamide

Peak value (δ) ppm	Peak type	No.of Hydrogen atoms assigned	Position in the structure
7.44	Doublet	1	1
7.51-7.55	Triplet	2	2
8.10	Doublet	2	3
7.60-7.65	Triplet	1	4
6.71-6.74	Doublet	1	5
7.03	Doublet	1	6
5.18	Singlet	2	7
12.51	Singlet	1	8

3.1.2.3^{13}C- NMR-ANALYSIS

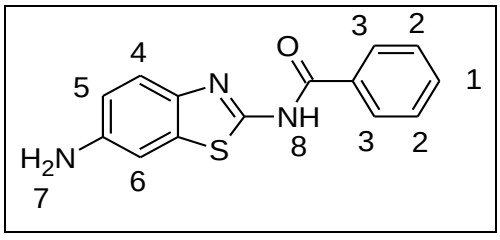

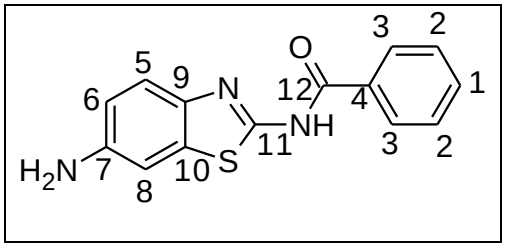

Figure. 11A Structure of N-(6-nitrobenzo[d]thiazol-2-yl) benzamide for ^{13}C- NMR analysis

Figure 11B Structure of N-(6-aminobenzo[d]thiazol-2-yl) benzamide for ^{13}C- NMR analysis

3.1.2.3.1 ^{13}C-NMR-ANALYSIS OF N-(6-nitrobenzo[d]thiazol-2-yl)benzamide

The ^{13}C NMR spectral data of N-(6-nitrobenzo[d]thiazol-2-yl)benzamide are presented in Table 8. The recorded spectrum was shown in Figure 12A..The singlet at 118.9 ppm is assigned to one carbon labeled as 8, singlet at 120.4 ppm is attributed to one carbon labeled as 6, singlet at 121.7 ppm is referred to one carbon is assigned to carbon labeled as 5, singlet at 128.44 ppm is assigned to one carbon labeled as 11, singlet at 128.49 ppm is referred to one carbon is assigned to carbon labeled as 1, singlet at 128.6 ppm is related to two carbon is assigned to carbon labeled as 2, singlet at 129.19 ppm is ascribed to two carbon labeled as 3, singlet at 131.3 ppm is referred to one carbon is assigned to carbon labeled as 4, singlet at 133.1 ppm is attributed to one carbon labeled as 10, singlet at 143.0 ppm is attributed to carbon atom labelled as 7, singlet at 164.21 ppm is assigned to carbon atom labelled as 12 and singlet at 166.3 ppm is attributed to carbon atom labelled as 9 .

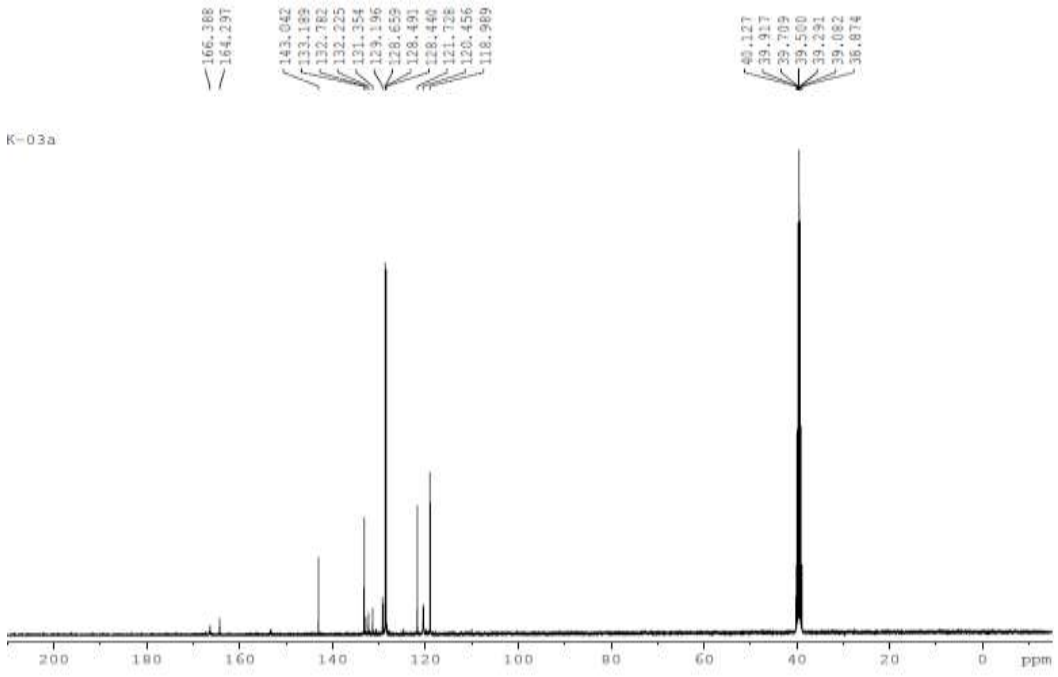

Figure 12A. ^{13}C- NMR spectrum of N-(6-nitrobenzo[d]thiazol-2-yl)benzamide

Table 8. ^{13}C-NMR spectral data of N-(6-nitrobenzo[d]thiazol-2-yl)benzamide.

Peak value	Peak type	No: of carbon assigned	Position in the structure
118.9	Singlet	1	8
120.4	Singlet	1	6
121.7	Singlet	1	5
128.44	Singlet	1	11
128.49	Singlet	1	1
128.6	Singlet	2	2
129.19	Singlet	2	3
131.3	Singlet	1	4
133.1	Singlet	1	10
143.0	Singlet	1	7
164.21	Singlet	1	12
166.3	Singlet	1	9

3.1.2.3.2 ^{13}C-NMR-analysis of N-(6-aminobenzo[d]thiazol-2-yl)benzamide

The ^{13}C NMR spectral data of N-(6-aminobenzo[d]thiazol-2-yl)benzamide are presented in Table 9. The recorded spectrum of the synthesized compound was shown in Figure 12B. The singlet at 103.9 ppm is assigned to one carbon labeled as 8, singlet at 114.5 ppm is attributed to one carbon labeled as 6, singlet at 120.6 ppm is referred to one carbon is assigned to carbon labeled as 5, singlet at 128.08 ppm is assigned to two carbon labeled as 3, singlet at 128.51 ppm is referred to two carbon is assigned to carbon labeled as 2, singlet at 132.19 ppm is ascribed to one carbon labeled as 1, singlet at 132.50 ppm is attributed to one carbon labeled as 4, singlet at 132.97 ppm is referred to one carbon is assigned to carbon labeled as 10, singlet at 139.4 ppm is attributed to one carbon labeled as 9, singlet at 145.89 ppm is attributed to one carbon atom labeled as 7, singlet at 153.79 ppm is assigned to carbon atom labeled as 12 and singlet at 165.26 ppm is assigned to one carbon atom labeled as 11. The structure of the N-(6-aminobenzo[d]thiazol-2-yl)benzamide was evidently confirmed using the resulting data

Table 9. ^{13}C- NMR spectral data of N-(6-aminobenzo[d]thiazol-2-yl)benzamide.

Peak value	Peak type	No: of carbon assigned	Position in the structure
103.9	Singlet	1	8
114.5	Singlet	1	6
120.6	Singlet	1	5
128.08	Singlet	2	3
128.51	Singlet	2	2
132.19	Singlet	1	1
132.50	Singlet	1	4
132.97	Singlet	1	10
139.4	Singlet	1	9
145.89	Singlet	1	7
153.79	Singlet	1	12
165.26	Singlet	1	11

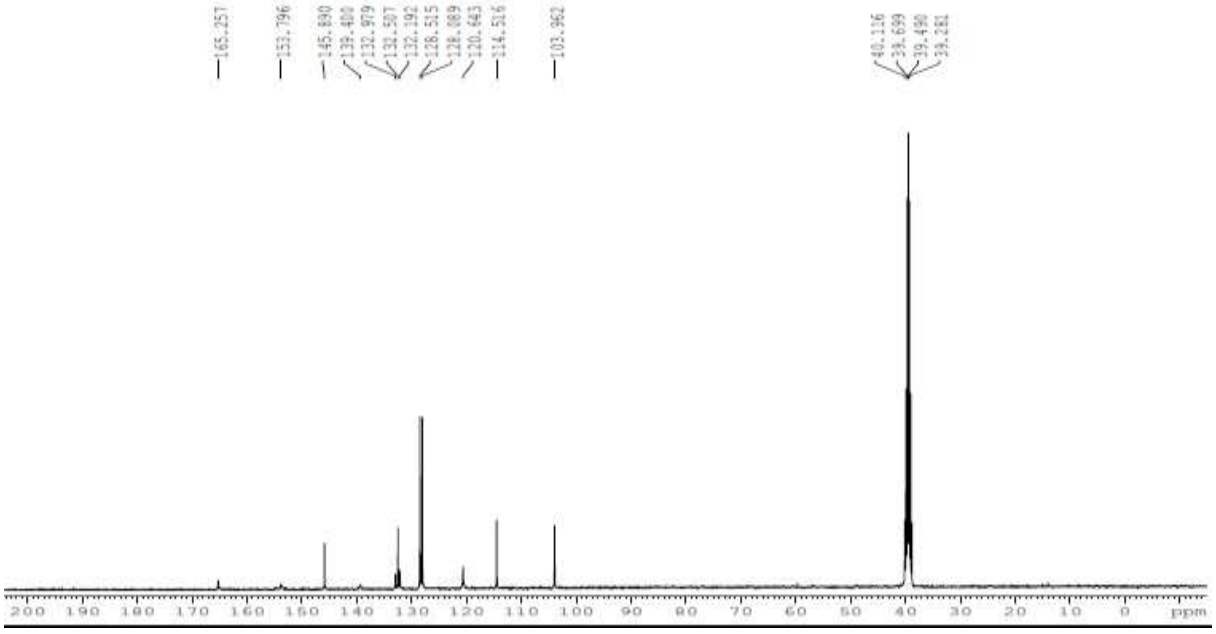

Figure 12B.^{13}C- NMR spectrum of N-(6-aminobenzo[d]thiazol-2-yl)benzamide

.

3.2 Corrosion measurements

3.2.1 Non-Electrical methods

Corrosion inhibition effect of all the synthesized organic compounds on mild steel corrosion in 1N HCl solution has been studied and the results obtained were calculated and discussed below.

3.2.1.1 Weight loss experiments:

Weight loss experiments were performed with different inhibitor concentration ranges for an immersion time of one hour in 1N HCl at 303K up to an optimum condition. The results about the present investigation of 2-amino-6-nitrobenzothiazole, 2, 6- diaminobenzothiazole and N-(6-aminobenzo[d]thiazol-2-yl)benzamide as corrosion inhibitor are tabulated and discussed according to different parameters studied.

Table 10: Effect of inhibitor concentration on mild steel corrosion in 1N HCl 30 ± 1 °c (weight loss method)

Concentration of the Inhibitor (ppm)	ANBT		DABT		ABTB	
	CR (Ɵ)	I.E (%)	CR (Ɵ)	I.E (%)	CR (Ɵ)	I.E (%)
	1130.49		1130.49		1130.49	1130.49
100	804.34	28.85	251.22	77.78	162.11	85.66
200	768.16	32.05	234.47	79.26	121.75	89.23
300	753.69	33.33	167.48	85.19	106.94	90.54
400	695.70	38.46	133.98	88.15	82.98	92.66
500	630.47	44.23	92.11	**91.85**	60.36	94.66
600	576.21	49.03	124.80	88.96	27.69	**97.55**
700	549.87	51.36	144.36	87.23	42.61	96.23

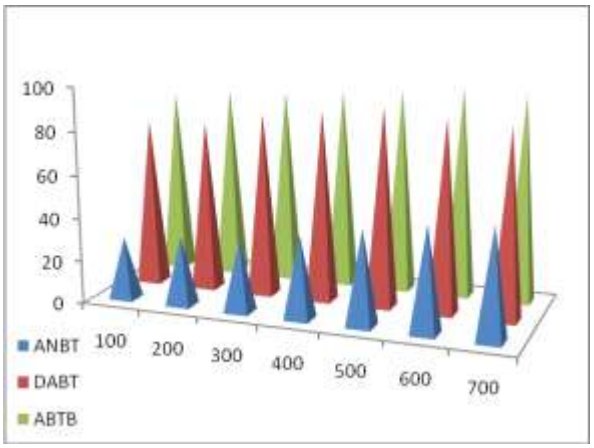

Figure13.Effect of concentration of the inhibitor

3.2.1.1.1 Effect of concentration of the inhibitor:

It can be seen from the Table10 and the Figure 13 that the inhibition efficiency of DABT and ABTB was greater when compared with that of 2-amino-6-nitrobenzothiaole. Since DABT and ABTB showed the better inhibition, we have studied the effect of the inhibitor for variation in time and concentration of inhibitor and acid.Table10 shows that the maximum inhibition efficiency of DABT was 91.85% at 500 ppm and ABTB was 97.55% at 600 ppm for HCl (1N) for an immersion time of 1hr, but the further rise in inhibitor concentration decreases the inhibition efficiency. Increase in surface coverage of increase the inhibition efficiency upto 500 ppm(DABT) and 600 ppm of ABTB inhibitor increase the presence of surface active compounds which accelerate the corrosion process[13,14]. At higher concentration due to sterric hindrance decrease the surface coverage, which results in reduced inhibition[15].

Table 11.Inhibition efficiency of DABT and ABTB on mild steel corrosion in 1N HCl at 303K for various time intervals and acid concentration

Inhibitor Conc (ppm)	IE(%) for variation in time and conc of inhibitor											
	DABT			ABTB			DABT			ABTB		
	1hr	3hr	5hr	1hr	3hr	5hr	1N	3N	5N	1N	3N	5N
100	77.78	81.25	84.65	85.66	88.55	89.55	77.78	47.23	34.95	85.66	80.66	75.44
300	85.19	88.24	90.45	90.54	92.66	93.45	85.19	56.49	41.65	90.54	85.59	82.65
500	**91.85**	**93.03**	**95.11**	94.66	96.56	96.9	**91.85**	**65.21**	**50.94**	94.66	89.65	85.55
600	88.96	90.28	93.27	**97.55**	**98.27**	**98.48**	88.96	64.91	48.16	**97.55**	**91.23**	**87.65**
700	87.23	89.67	91.67	96.23	97.48	97.69	87.23	60.78	39.71	96.23	88.64	86.11

3.2.1.1.2 Effect of immersion time:

From the Table 11 it can be seen that the maximum inhibition efficiency was 98.48% at 600ppm(ABTB) and 93.27% at 500ppm(DABT) for 5 hr and the film remains to be consistent with increase in immersion time upto 5 hours in both the inhibitor molecule but in some cases after longer immersion desorption of the inhibitor molecule coating from the metal surface takes place which increase the corrosion process[16]. In both the cases of the inhibitor molecule, the film was strongly adsorbed on the metal surface so with increase in immersion time; the film remains constant. Hence, both the inhibitor can be used for a longer time to prevent the metal from corrosion.

3.2.1.1.3 Effect of acid concentration:

The results revealed from Table11 showed that the protective layer formed by the added inhibitor protected the metal up to 1 N HCl after that the inhibition efficiency decreased with increase in the concentration of the acid[17] in both the cases. With the increase in acid concentration, the dissolution of the metal film gets increased and the increase in both the acidity and Cl^- ions concentration[18] increases the corrosion process.

Table 12. Effect of temperature on mild steel corrosion in 1N HCl

Inhibitor concentration (ppm)	Inhibition efficiency%							
	DABT				ABTB			
	303K	313K	323K	333K	303K	313K	323K	333K
100	77.78	79.59	76.33	72.33	85.66	87.89	84.69	76.32
200	79.26	83.22	81.23	77.56	89.23	90.56	87.62	80.55
300	85.19	88.21	84.66	82.64	90.54	92.56	89.26	83.25
400	88.15	92.87	88.49	84.95	92.66	93.55	90.55	87.26
500	**91.85**	**96.22**	**90.17**	**87.23**	94.66	95.64	92.64	90.33
600	88.96	94.66	89.01	87.01	**97.55**	**98.65**	**94.78**	**91.78**
700	87.23	95.46	90.56	86.71	96.23	97.66	95.66	89.64

3.2.1.1.4 Effect of temperature:

The samples were exposed to acidic media at specific temperature (303, 313, 323, 333 and 343K) for the duration of 1hr. Table 12. illustrates that the maximum inhibition efficiency observed was 96.22%(DABT) at 500 ppm and 98.65%(ABTB) at 600 ppm at 313K whereas with increase in temperature the inhibition efficiency was found to be shown in the Table 13 indicate that the energy barrier for corrosion reaction increased in the presence of inhibitor without changing the dissolution mechanism[19,20]. It is due to the fact that the protective films of the inhibitor protected the metal upto 313K after that the film starts to breakdown and desorption of inhibitor molecule from the metal surface takes place at higher temperature. The Ea values (calculated using Arrhenius plots (Figure 14) increases in the presence of inhibitor DABT and ABTB indicates the formation of physical or weak bonding between the molecules of the inhibitor and the mild steel surface. The negative value of ΔG^{o}_{ads} shown in Table 13 ensures the spontaneous absorption of inhibitor on mild steel and the stability of the adsorbed layer[19]. The values of ΔG^{o}_{ads} upto -20KJ mol^{-1} are consistent with physical adsorption i.e. electrostatic interactions between the charged molecules and the charged metal

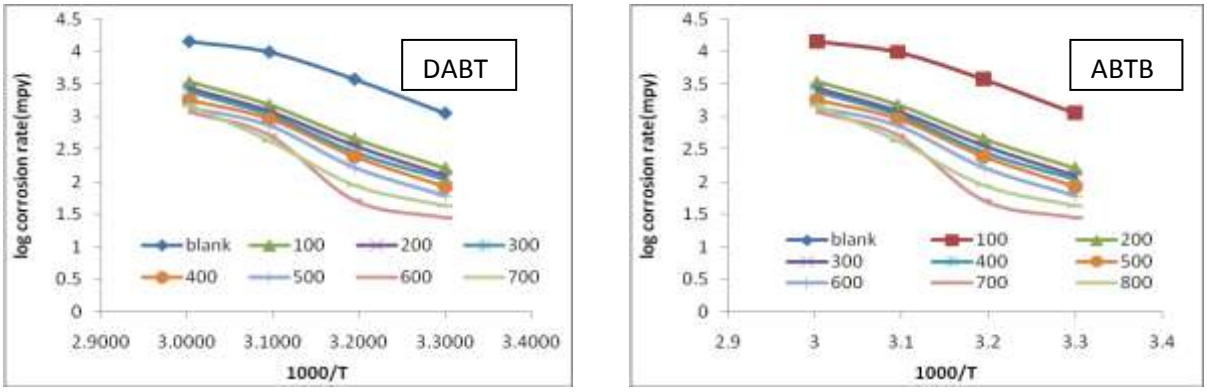

Figure 14. Arrhenius plot for corrosion of mild steel in 1N HCl solution in the absence and presence of inhibitor.

Table 13 .ΔG^{o}_{ads} KJ MOL^{-1} and Ea(calculated using arrhenius plot) for thecorrosion of mild steel in 1N HCl

Inhibitor Concentration (ppm)	-ΔG^{o}_{ads}KJ mol^{-1}								Ea	
	303K		313K		323K		333K		DABT	ABTB
	DABT	ABTB	DABT	ABTB	DABT	ABTB	DABT	ABTB	72.53	72.53
100	14.56	17.65	15.32	18.74	17.41	18.61	16.47	17.69	79.16	86.79
200	13.04	16.34	14.14	17.26	15.98	17.00	15.05	16.04	75.24	89.36
300	13.04	15.81	14.16	17.01	15.28	16.47	14.82	15.56	78.54	89.62
400	12.95	15.84	14.83	16.73	15.21	16.15	14.86	15.72	82.14	89.37
500	13.45	16.02	16.02	17.11	15.62	16.16	14.76	15.84	91.29	91.60
600	12.13	17.65	14.58	19.82	15.63	16.71	13.52	15.88	82.19	113.75
700	11.32	16.18	13.65	17.99	12.98	16.85	12.31	14.79	80.21	102.42

3.2.1.1.5 Adsorption isotherm:

Both the inhibitors obey Langmuir and Temkin adsorption isotherms(Figure 15 and 16) which confirm that the organic molecules are attached to the metal and prevent the contact the metal surface and the acid medium[11].

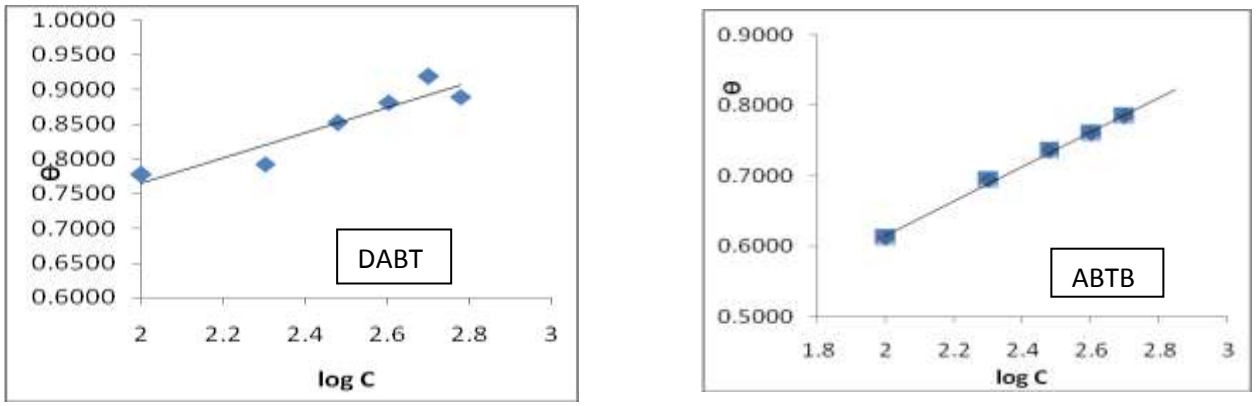

Figure 15 Temkin plot for the inhibitors

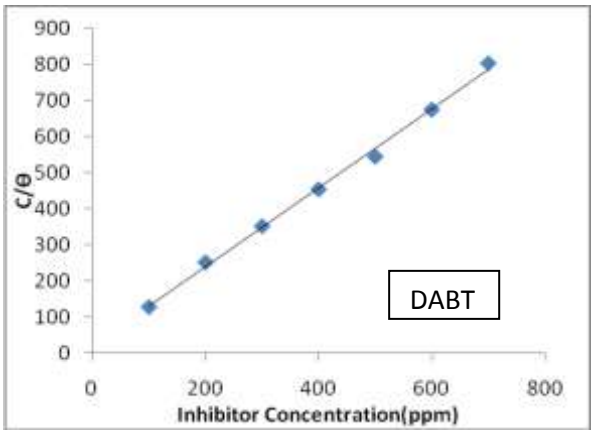

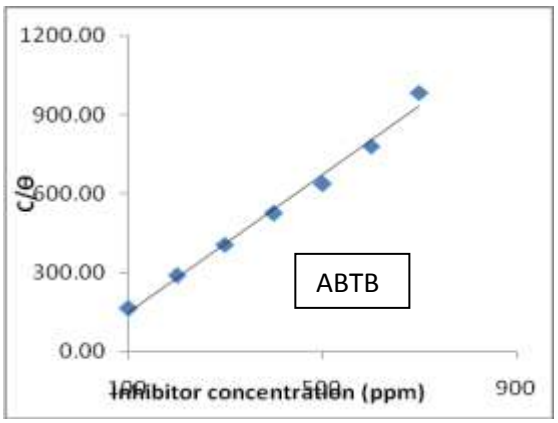

Figure 16 Langmuir plot of the inhibitors.

3.2.2.Electrical methods

3.2.2.1 Polarisation studies:

The corresponding polarization data (ba, bc, Ecorr, Icorr) are recorded in Table 14. In HCl medium, the Ecorr value is shifted in the noble direction in the presence of both the inhibitors. Further the Tafel slopes ba and bc both are decreased to the same extent. Both the inhibitor can be regarded as mixed type indicating that the inhibitor controlled both anodic dissolution and cathodic hydrogen evolution [21].The maximum inhibition efficiency obtained was 94.49% at 600ppm for DABT and 85.86% at 500ppm for ABTB for in 1N HCl.

Table 14.Corrosion parameters of mild steel in 1N HCl with DABT and ABTB by polarisation method

Conc of the inhibitor (ppm)	ba(V/dec)		bc(V/dec)		$E_{corr(mV)}$		$I_{corr}(mA/cm^2$		IE(%)	
	DABT	ABTB	DABT	ABTB	DABT	ABTB	DABT	ABTB	DABT	ABTB
Blank	7.153	7.153	6.308	6.308	-475		8.774			
100	7.947	8.099	6.567	7.694	-496	-505	2.751	1.303	68.88	85.44
200	8.394	8.083	6.776	7.862	-500	-508	1.768	0.9714	80.12	89.23
300	7.419	8.122	6.156	8.215	-514	-509	1.663	0.828	81.32	90.87
400	8.713	7.794	7.068	8.284	-504	-513	1.327	0.734	85.17	91.94
500	8.325	8.65	6.692	8.56	-510	-512	1.266	0.63	**85.86**	93.13
600	8.052	9.15	6.784	8.772	-518	-508	1.378	0.5115	84.58	**94.49**
700	7.839	9.64	6.249	8.594	-514	-511	1.389	0.5128	84.45	94.47

3.2.2.2 AC Impedance:

The anticorrosive performance of the inhibitor was also studied by electrochemical impedance spectral studies at 30±1°C for various concentrations of inhibitor in 1N HCl. The datas obtained are given in Table 15.The R_{ct} values were found to be increased in the presence of inhibitors. The double layer capacitance C_{dl} values decreased, as concentration increased. This decrease may be due to the adsorption of the compounds on the metal surface leading to a film formation. The corresponding Nyquist plot for the inhibitor in 1N HCl is shown in Figure18A & 18B. As can be noticed, the impedance diagrams are perfect semi-circles indicating a charge transfer process mainly controlling the corrosion of steel [22]. The maximum inhibition efficiency was found to be 72.58% at 500ppm for DABT and 86.65% at 600ppm for ABTB in 1N HCl.

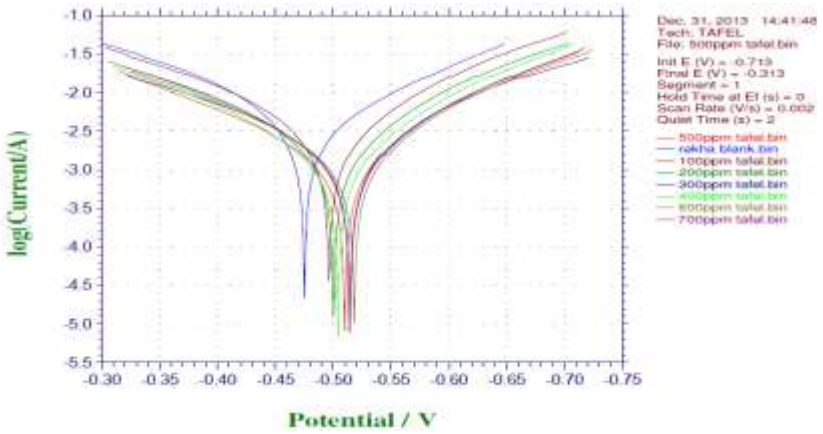

Figure 17A Potentiodynamic polarization curves for mild steel in 1N HCl with DABT

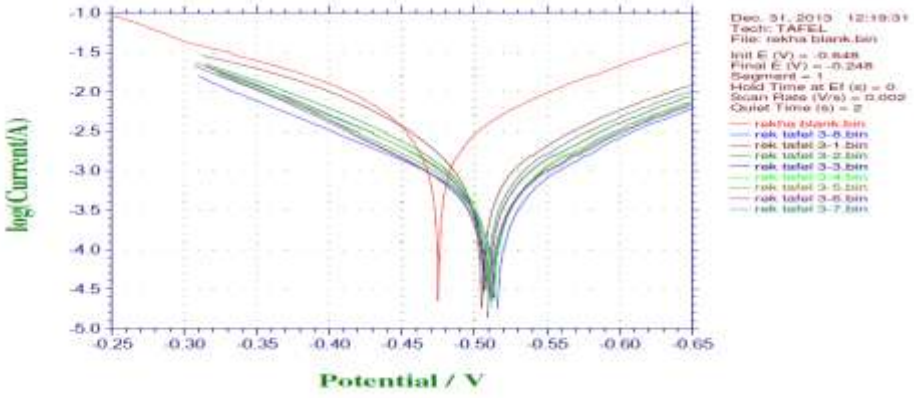

Figure 27 B Potentiodynamic polarization curves for mild steel in 1N HCl with ABTB

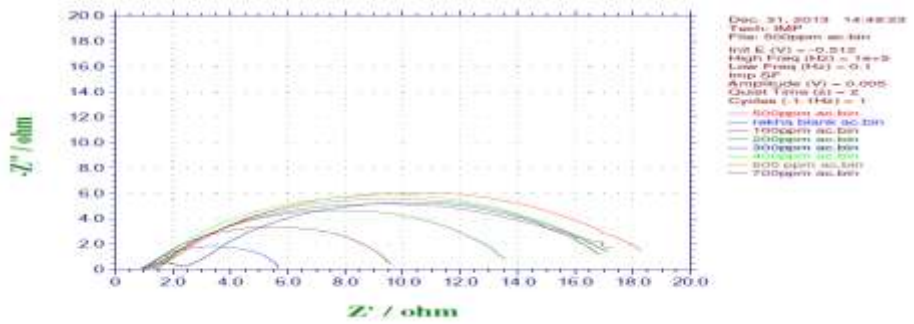

Figure 18A Nyquistic plot for mild steel in 1N HCl with DABT

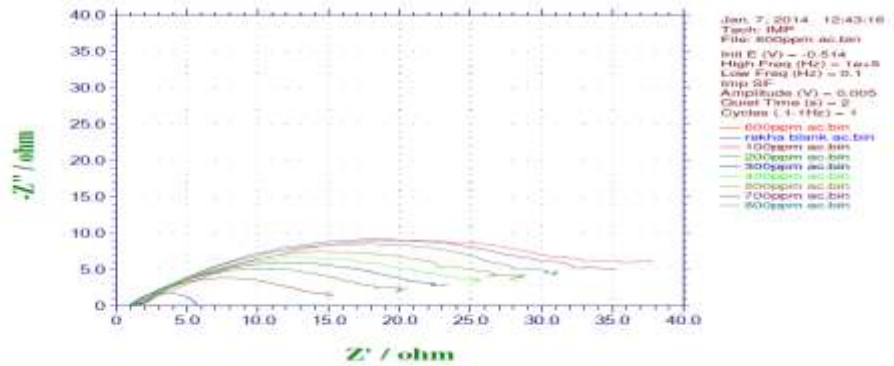

Figure 18B Nyquistic plot for mild steel in 1N HCl with DABT

Table 15.Corrosion parameters of mild steel in 1N HCl with DABT and ABTB by AC impedance method

Conc of the Inhibitor (ppm)	Rct(ohm.cm2)		C_{dl}(mV vs SCE)X10^{-5}		IE(%)	
	DABT	ABTB	DABT	ABTB	DABT	ABTB
Blank		4.75		596.18		
100	8.75	13.73	475.25	149.41	45.69	65.41
200	12.55	19.51	485.86	140.47	62.17	75.65
300	15.49	22.5	393.84	125.81	69.34	78.9
400	16.22	24.75	376.05	119.79	70.72	80.81
500	17.32	27.82	352.23	114.39	**72.58**	82.93
600	16.43	30.06	371.2	100.37	71.1	**86.65**
700	16.31	29.2	373.94	142.3	70.89	86.1

3.3. Surface Analysis

3.3.1. Scanning Electron Micrograph:

The surface morphology of the inhibitor molecule on the mild steel specimen was studied using SEM technique. The SEM micrograph (Figure 19A, B and C) of the mild steel in 1 N HCl in the presence and absence of DABT and ABTB. Figure 19A shows that the metal surface consists of many pits in the absence of an inhibitor molecule but in the Figure 19B and 19C shows no evidence of pitting but shows a protective film like surface. This protective film blocks the active sites present on the mild steel surface and inhibits the corrosion process.[23].

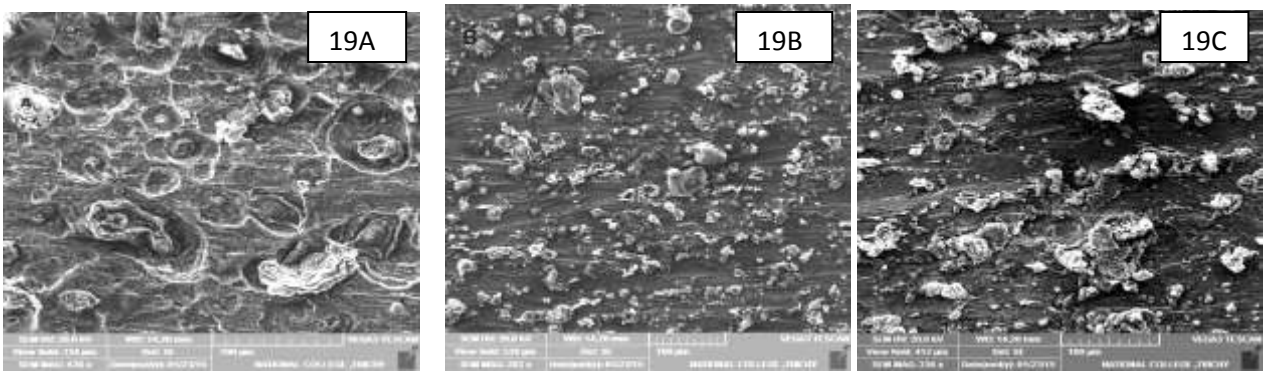

Figure 19 A. SEM of Mild steel in 1N HCl without inhibitor . 19B. SEM of Mild steel in 1N HCl with 2,6 Diaminobenzothiazole 19 C. SEM of Mild steel in 1N HCl with N-(6-aminobenzo[d]thiazol-2-yl) benzamide

3.3.2 .IR studies.

FT-IR spectrum of mild steel in 1N HCl with and without DABT are shown in Figure 20A and 20B. The corresponding peak values are given in Table 16. The broad peak appeared in the region of 3386.76 cm^{-1} is due to the presence of superficial adsorbed water corresponding to stretching mode of an OH. The peaks appeared in the region of 3098 cm^{-1}, 1547.58 cm^{-1}, and 798.87 cm^{-1} were shifted to 3120.05 cm^{-1}, 1550.61cm^{-1} and 814.62 cm^{-1} which show that the electronic cloud and the double bond in the aromatic molecule involves in the formation of the surface film which retards the corrosion process. The stretching frequency of amine shifts from 1613.37 cm^{-1} to 1598.34 cm^{-1} which are due to the lone pair of electrons present in nitrogen atom tends to co-ordinate with Fe^{2+} to form Fe- DABT complex.

FT-IR spectrum of mild steel in 1N HCl with and without ABTB are shown in Figure 20A and 20C. The corresponding peak values are given in Table 16. The broad peak appeared in the region of 3386.76 cm^{-1} is due to the presence of superficial adsorbed water corresponding to stretching mode of an OH. The stretching frequency of amine and amide 3399.60 cm^{-1}, 3321.33 shifts to 3402.37cm^{-1}as a broad peak which is due to the lone pair of electrons present in nitrogen atom tends to co-ordinate with Fe^{2+} to form Fe- ABTB complex. The peaks appeared in the region of 3063.47 cm^{-1}, 1464.72 cm^{-1}, and 698.03 cm^{-1} were shifted to 2803.47 cm^{-1}, 1469.94cm^{-1} and 698.36 cm^{-1} which show that the electronic cloud and the double bond in the aromatic molecule involves in the formation of the surface film which retards the corrosion process. The stretching frequency of the carbonyl group shifts from 1659.05 to 1595.31 due to electron cloud density shifts from oxygen atom to co-ordinate with Fe^{2+} to form Fe- ABTB complex. The film formation is due to the interaction of oxygen; nitrogen atoms present in DABT and ABTB with Fe in mild steel thereby Fe- DABT and Fe-ABTB complex was formed. It retards the corrosion process[23].The peaks appeared between the ranges of 400-700cm cm^{-1} are mainly due to Fe_2O_3.

ISSN 2321-807X
Volume 12 Number12
Journal of Advances in chemistry

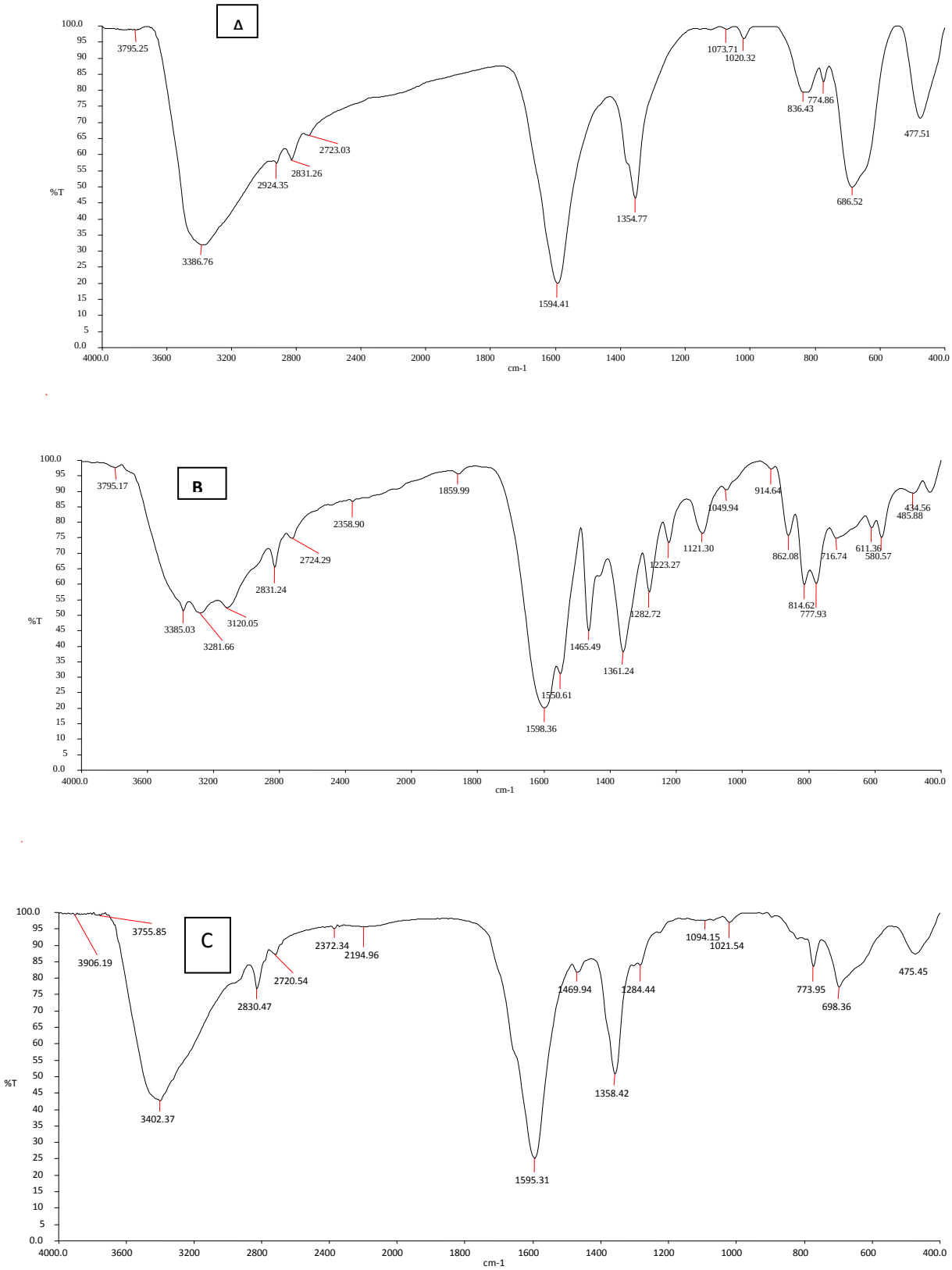

Figure 20A FT-IR spectrum of Mild steel in 1N HCl without inhibitor . 20B. FT-IR spectra of Mild steel in 1N HCl with 2,6 Diaminobenzothiazole 19 C. FT-IR spectra of Mild steel in 1N HCl with N-(6-aminobenzo[d]thiazol-2-yl) benzamide

Table 16 FT-IR Peak Value(cm^{-1}) of N-(6-aminobenzo[d]thiazol-2-yl)acetamide, Mild steel in 1N HCl and Mild steel in 1N HCl with inhibitor

S.no	FT-IR Peak Value(cm^{-1})			Possible groups	FT-IR Peak Value(cm^{-1})		Possible groups
	Mild steel in 1N HCl	DABT	Mild steel in 1N HCl with inhibitor		ABTB	Mild steel in 1N HCl with inhibitor	
1	3386.76	-	3385.03	υO-H	3399.60	3402.37	Amine
2	-	3098	3120.05	Aromatic=CH (stretching)	-		υO-H
3	1594.41	-	1598.34	∂HOH	3321.33	3402.37	Amide
4	-	1613.37	1598.34	1° amine	3063.47	2830.47	–C-H- group in the aromatic ring
5	-	1547.58	1550.61	Aromatic C=C(stretching),	1659.05	1595.31	C=O attached to amidegroup
6	686.52	-	716.74	γ OH	-	1595.31	∂HOH
		798.87	814.62	=CH (bending)	1464.72	1469.94	–C=C- group in the aromatic ring
7	477.51	-	485.88	γ FeO			γ OH
					698.03	698.36	Aromatic monosubstitution (C-H deforming)
						475.45	γ FeO

CONCLUSION

The following are the conclusions made from the studies

1. DABT and ABTB exhibit excellent inhibition efficiency towards corrosion of mild steel in1N HCl.
2. The optimum inhibition efficiency was 91.85% at 500ppm for DABT and and 97.55% at 600 ppm for ABTB for one hour of immersion in 1N HCl.
3. The optimum inhibition efficiency was 98.65% at 600ppm(ABTB) and 96.22% at 500ppm(DABT) for at a temperature of 40ºC for an immersion of 1 hour in 1N HCl
4. The optimum inhibition efficiency was 98.48% at 600ppm (ABTB) and 93.27% at 500ppm (DABT) for 5 hr of immersion in 1 N HCl.
5. The adsorption of the inhibitor on the mild steel follows physisorption mechanism.
6. The process of adsorption of the inhibitor molecule on the mild steel surface obeys Langmuir and Temkin adsorption isotherm.
7. Potentiodynamic polarization studies show that Icorr values decreased upto 500ppm for DABT and 600 ppm for ABTB then increased and the shifts in b_a, b_c, E_{corr} suggested that the inhibitor acts as a mixed type.
8. AC impedance studies revealed that the corrosion process of metal is controlled by charge transfer process.
9. SEM proves the formation of smooth, dense protective layer in the presence of an effective inhibitor.
10. FT-IR analysis of the surface film indicates the formation of Fe-ABTB and Fe-DABT complex which retards the corrosion process.

REFERENCES

1. O. James, N.C. Oforka and O.K. Abiola, Int. J. Electrochem. Sci. 2(2007) 278.
2. M.A. Quraishi and H.K. Sharma, Mater. Chem. Phys. 78 (2003)18.
3. N. Pebere, M. Duprat, F. Dabosi, A. Lattes and A. De Savignac , J. Appl. Electrochem.18 (1988) 225.
4. F. Bentiss, M. Lagrenee,M. Traisnel and J.C. Hornez, Corros. Sci. 41(1999)789.
5. K.F. Khaled, Electrochim. Acta. 48(2003) 2493.
6. H. Shokry, M. Yuasa, I. Sekine, R.M. Issa, H.Y. El-Baradie, G.K. Gomma, Corros.Sci. 40(1998)2173..
7. K.C.Emregul and O.Atakol, Mater. Chem. Phys. 82(2003)188.
8. Y.Li, P. Zhao, Q. Liang and B.R.Hou, Appl. Surf. Sci. 252(2005)1245.
9. E.A. Noor, Corros. Sci. 47(2005)33.
10. K.Parameswari, S. Rekha and S.Chitra, J. Basic.Appl.Chem. 1(2011)39.

11. K.Parameswari,S.Rekha ,S.Chitra and E.Kayalvizhy, Port.Electrochim Acta.28(2010)189.
12. M.A. Quraishi, M.A. Wajid Khan and M. Ajmal, J. Appl. Electrochem. 26(1996)1253.
13. S.T. Keera, J SCI IND RES 62(2003)188.
14. T.Vasudevan, Corros Sci. 37(1995)1235.
15. S.T. Keera, A.A. Mohamed and A.M. Badawi, Egypt J Petrol. 10, 2 (2001)
16. V.G. Vasudha and K. ShanmugaPriya, Res.J.Che. Sci. 3(2013)21.
17. M.A. Quraishi, and Sudhish Kumar Shukla.:,Materials Chemistry and Physics. 113(2009)685.
18. E.A. Noor and A.H. Al-Moubaraki, Electrochem. Sci. 3(2008)806.
19. M.Mobin and SheerinMasroor.: ,Int. J. Electrochem. Sci. 7(2012)6920.
20. H. Ashassi-Sorkhabi, B.Shaabani and D.Seifzadeh, Appl. Surf. Sci. 239(2005)154.
21. A.Y. Musa, A.A.H. Kadhum, A.B.Mohamad, A.R.Duad, M.S.Takriff and S.K. Kamarudin, ,Corros. Sci. 51(2009)2393.
22. Ramesh SaliyanV.; AirodyVasudevaAdhikari: IndianJ.Chem.Technol. 16(2009)162.
23. P. Thiraviyam and K. Kannan, Arab J Sci Eng. 38(2013)1757.